Interdiffusion and chemical trapping at InP(110) interfaces with Au, Al, Ni, Cu, and Ti

Yoram Shapira* and L. J. Brillson
Xerox Webster Research Center, Webster, New York 14580

A. D. Katnani and G. Margaritondo
Physics Department, University of Wisconsin—Madison, Madison, Wisconsin 53706
(Received 15 March 1984)

We have studied UHV-cleaved (110) surfaces of InP covered with a large variety of metal layers and interlayers, using Auger-electron spectroscopy in conjunction with Ar^+-ion sputtering. All measurements were made under identical experimental conditions, other than the thickness or type of the metal films, in order to minimize ion-beam-induced distortion of the data. We find that In and especially P are segregated at unreactive metal surfaces such as Au or Cu. Very thin interlayers of "reactive" metals between Au and InP completely reverse the out-diffused distribution of the phosphorus, which is accumulated at the interface due to chemical trapping by the reactive-metal interlayers. Indium out-diffusion is found to be unaffected by these interlayers while Au in-diffusion depends sensitively on the type of metal interlayer. The results are correlated with soft-x-ray photoemission spectroscopy (SXPS) measurements to reveal the diffusant spatial distribution on a microscopic scale while illustrating the relative limitations of the SXPS technique. The contrasting effects of the unreactive versus reactive-metal interfaces are correlated with Schottky-barrier heights and with energy-level calculations of associated surface defects.

I. INTRODUCTION

Recently, there has been considerable interest in InP both as a prototypical III-V compound suitable for basic studies and a potential candidate for a variety of electronic and optoelectronic devices. The feasibility of various useful devices, such as metal-insulator semiconductor field-effect transistors[1–4] (MISFET's) for high-speed applications, Schottky diodes,[5] solar cells,[6] and photoelectrochemical cells,[7] based on InP has been extensively demonstrated. Understanding and knowledge about the electronic and chemical properties of InP surfaces and metal interfaces are of major technological importance for improving the performance of such devices. Experimental work in this direction have used a wide variety of techniques for electrical,[8,9] electronic,[10,11] compositional,[12,13] and structural[14] analyses of InP surfaces[15,16] and interfaces.[17] The experimental techniques comprised *I-V* (Ref. 18) and *C-V* (Ref. 19) measurements, ultraviolet, soft-x-ray, and x-ray photoelectron spectroscopies[12–14] (UPS, SXPS, and XPS, respectively), low-energy electron diffraction[20] (LEED), Auger-electron spectroscopy (AES), and sputter profiling[21–23] and surface photovoltage spectroscopy.[24]

The data reveal that the metal-InP interface is not abrupt.[9,25,26] Instead, a number of phenomena occur upon metal deposition including interdiffusion,[13] reactions which create new interfacial compounds,[26] defect formation,[9,25] and removal or addition of gap surface states.[11] These phenomena depend very sensitively on the reactivity of the deposited metal and can be dramatically altered by extremely thin interlayers of different metals.[10] In turn, these interfacial processes and properties seem to be crucial in determining the Schottky-barrier height observed at such interfaces. An extremely important task that remains is to find a correlation between the interfacial properties of InP and its electrical characteristics, and possibly to extend it to compound semiconductors in general.

In this paper we present results of an extensive study of InP(110) surfaces covered with thin films and interlayers of various metals with different thicknesses. We have endeavored to find a general pattern of anion and cation out-diffusion and metal-atom in-diffusion as a function of metal type and thickness. We have kept all other experimental parameters unchanged in order to cancel out any inherent artifacts and causes of misinterpretation due to the sputtering process. Thus, we were able to probe the InP-metal interfaces *post factum* and compare the results with UPS and SXPS data,[12–14,25,26] which are taken at very low metal coverages during the build-up of the junction. The experimental techniques we have used are described in Sec. II. In Sec. III we present the experimental results, which describe well-characterized patterns of redistribution of the semiconductor and metal constituents at the interfaces as well as the metal surface due to interdiffusion and reaction, depending on the reactivity of the metal layer or interlayer. These results are discussed in Sec. IV and compared with other results and theoretical predictions.

II. EXPERIMENTAL

The InP crystals studied were supplied in the form of $(5\times5\times15)$-mm^3 bars with $p=4.3\times10^{15}$ cm^{-3} (Zn) by MCP Electronic materials (Alperton, Middlesex, England). These were cleaved in a UHV system with a base pressure $\leq5\times10^{-11}$ Torr to expose visually smooth (110)

 ©1984 The American Physical Society

surfaces. These surfaces were covered with metal layers by deposition from shielded W-filament sources at pressures in the low-10^{-9}-Torr range. The deposition thickness was monitored by a quartz-crystal oscillator. The surfaces were then analyzed by AES using a double-pass cylindrical mirror analyzer (CMA) and a grazing-incidence electron gun. All spectra were acquired with a 2-keV electron-beam energy and 2-eV CMA modulation voltage. Electron current was restricted to ≤ 2 μA focused on a 0.1-mm-diam spot in order to minimize electron-beam effects. For sputter profiling, we used a grazing-incidence Ar^+-ion gun operated at 2×10^{-4} Torr Ar pressure (system Ar-background pressure $\leq 3\times 10^{-8}$ Torr), 25-mA emission current, and 1-keV beam energy, which was typically rastered over a (4×4) mm^2 area on the sample. The electron beam was directed to the center of the rastered area. Each spectrum was obtained by signal-averaging for 100 sec, during which the sputtering rate (for Au) was estimated to be about three monolayers (ML).

Mild annealing (200 °C) was carried out using a focused quartz halogen lamp external to the chamber. We also performed angle-integrated SXPS experiments using synchrotron radiation at the University of Wisconsin Synchrotron Radiation Center and a double-pass CMA in a similar UHV chamber.

III. RESULTS

Figure 1 shows an Auger-electron spectrum of a typical UHV-cleaved (110) surface of InP. There are no traces of contaminants on the surface. However, the P:In peak-to-peak (p.-p.) height ratio is much higher than the one shown in Fig. 2 which was obtained from the same crystal after prolonged Ar^+-ion bombardment. Figure 3 is a depth profile of the In and P atomic concentrations as a function of sputtering time. There is a sharp change at the surface, followed by a slower decrease (increase) of the P (In) peak-to-peak height. The latter is evidence of the phosphorus preferential sputtering,[22] but the topmost-layer behavior is a strong indication of a P-rich surface produced by the cleavage. This is further supported by surface photovoltage measurements[11] and by comparison with InP(100) surfaces.[24] After Ar^+-ion sputtering of the cleaved surface, a constant I_{In}/I_P peak-to-peak height ratio is achieved. Only in Fig. 3 was the relative I_{In}/I_P Auger sensitivity taken to match In and P intensities after prolonged sputtering. Taking the subsurface as representative of the clean, stoichiometric InP, we have adjusted the relative I_{In}/I_P Auger sensitivity accordingly and used the new sensitivity ratio to normalize all subsequent depth profiles.

Figure 4 shows a typical Auger-electron spectrum obtained from a 30-Å-thick Au film deposited on a UHV-cleaved (110) surface. In addition to the Au peak, In and P peaks are also present. No other peaks can be detected. These AES Au, P, and In p.-p. heights were recorded as a function of sputtering time, during 1-keV Ar^+-ion bombardment of a (4×4)-mm^2 area. The normalized depth profiles obtained from five different thicknesses of Au films are shown in Fig. 5. Sputtering and AES parameters are identical for all the interfaces shown. Several points should be noted: (1) As the Au film thickness is increased, a redistribution pattern emerges, which indicates

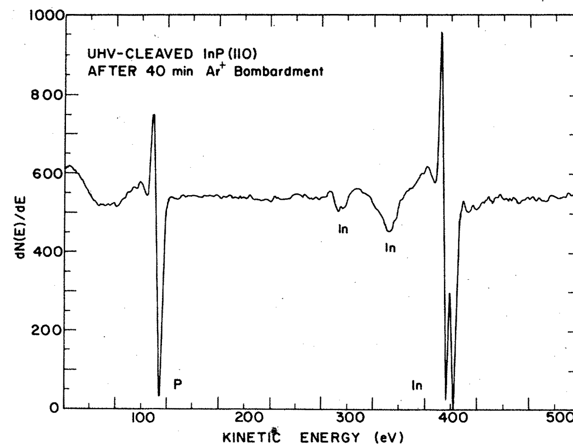

FIG. 2. AES features taken under same experimental conditions and from same sample as in Fig. 1 after 40 min of Ar^+-ion bombardment (after a constant I_{In}:I_P p.-p. ratio had been achieved).

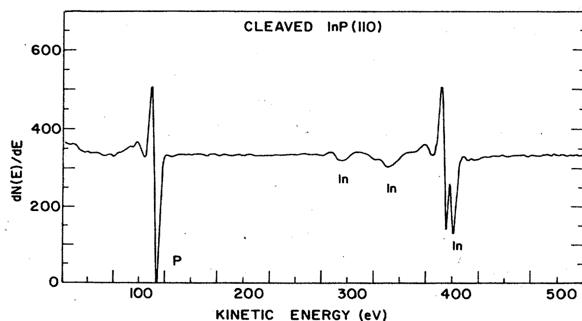

FIG. 1. AES features of a UHV-cleaved InP(110) surface taken with a 2-keV, 2-μA electron beam focused to a 0.1-mm-diam spot and 2-eV CMA modulation.

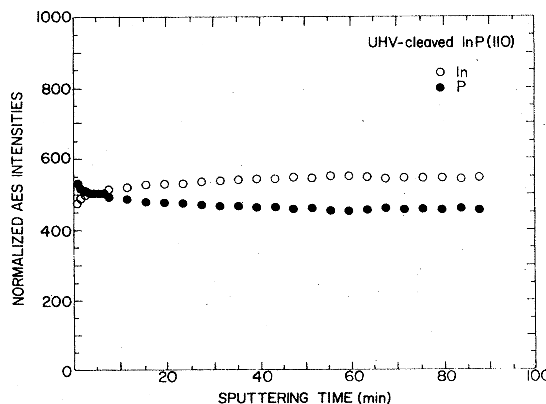

FIG. 3. Normalized AES intensities of P (solid curve) and In (dashed curve) as a function of sputtering time taken from an initially UHV-cleaved InP(110) surface.

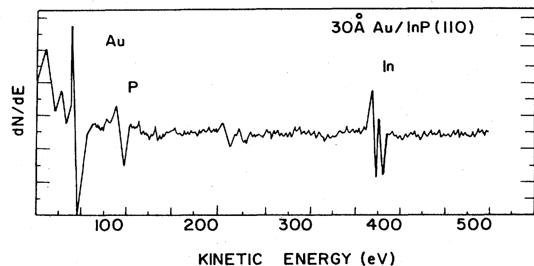

FIG. 4. AES features taken from 30-Å-thick Au film deposited on a UHV-cleaved InP(110) surface. AES parameters same as in Fig. 1.

a strong P and In segregation at the free-metal surface, small In and no P concentration within the film (in accordance with their solid solubilities[27]), and a nonabrupt interface. (2) The phosphorus surface segregation is up to a factor of 2 higher than the In. (3) The bulk In peak precedes the bulk P peak when the interface is approached. This is due to the fact that the In *MNN* electrons have a larger escape depth than the P *LMM* electrons. However, this effect is superimposed on the In excess (or P deficiency) induced at the interface by the Au deposition. Results presented later point to this interface redistribution of P as the origin of the segregated P at the metal surface. (4) The segregated layer is not apparent at Au thicknesses below 30 Å, which may indicate that 10 or 20 Å are below a typical threshold thickness for segregation or, more probably, that at such thin layers the transition from the segregated layer to the substrate semiconductor is masked by the inherent escape depth of the Auger electrons and the width of the disordered layer caused by the sputtering. We estimate that 10–20 Å represent a characteristic depth resolution of the results. (5) The Au signal is detectable after the In and P signals seem to have reached their bulk values. This indicates gold in-diffusion simultaneously with In and P out-diffusion, a process which is confirmed by results presented later. (6) The segregated layer shows an almost constant P concentration, while the In concentration seems to decrease, with increasing Au thickness. We estimate the segregated P layer to be about 10 Å thick. These results suggest a "floating" process of the excess surface P on top of the Au film being deposited.

In order to gain insight into the microscopic details of the latter process, SXPS measurements were carried out under similar experimental conditions. Figure 6 shows a photoemission spectrum for the In 4*d* levels for increasing Au coverage of UHV-cleaved InP(110) surface. We have used a photon energy of 70 eV in order to obtain maximum surface sensitivity, analyzing photoelectrons with 50 eV kinetic energy which have a minimal escape depth. Indeed, the spectra show that starting at Au coverages above a monolayer, the In 4*d* core level exhibits an initial 0.9-eV shift to lower binding energies while retaining its spin-orbit splitting. This shift is in good agreement with other Au-InP results.[28] Further Au deposition causes an additional shift until stabilization of the level at 1.05 eV below the cleaved binding-energy state. Such shifts are

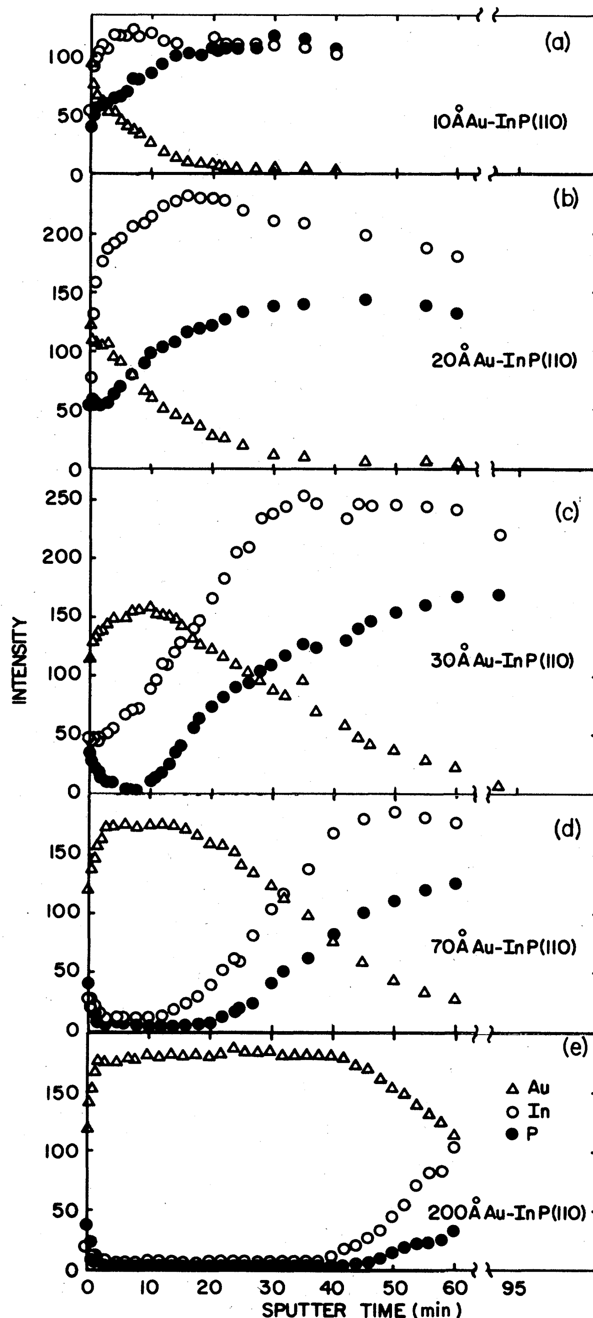

FIG. 5. AES, Au, In, and P depth profiles for different Au-overlayer thicknesses on a UHV-cleaved InP(110) surface. Sputtering conditions were identical throughout the profiles for all five interfaces. Ion-beam-raster dimensions were 4×4 mm^2.

due to both band bending and chemical-bonding change. Specifically, the results indicate that Au deposition causes dissociation of the In—P bonds, while covering the surface with a continuous layer of Au intermixed with metallic In and P atoms. This is confirmed by the absence of an unshifted In 4*d* peak. Thus it seems that some of the dissociated In and P, including the initial excess P, segregate to the top of the deposited layer. The rest remains at the interface, creating the concentration gradient from the InP

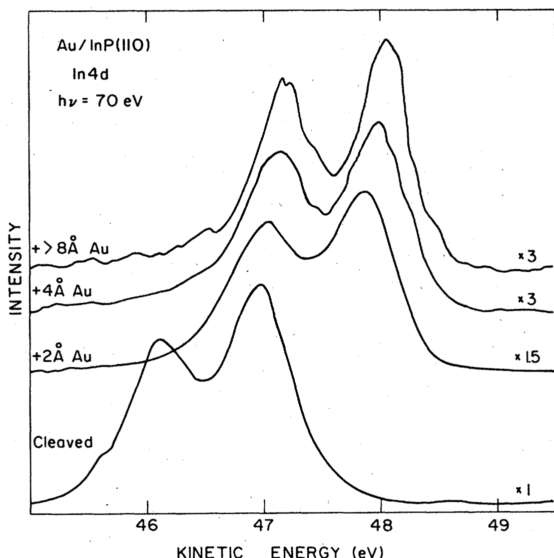

FIG. 6. Soft-x-ray photoemission spectra of the In $4d$ core level as a function of increasing Au deposition on a UHV-cleaved InP(110) surface using $h\nu = 70$ eV.

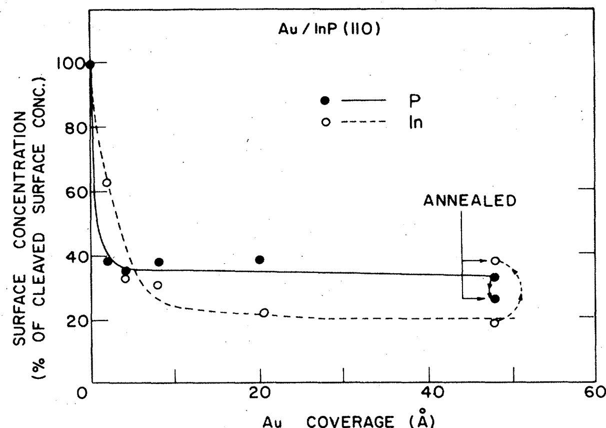

FIG. 7. Surface concentration of In (open circles) and P (solic circles) (in percent of cleaved-surface In $4d$ and P $2p$ peak areas as a function of increasing Au coverage using $h\nu = 70$ and 17ͩ eV, respectively.

substrate to the level soluble in the Au film.

These processes may be supported by Fig. 7, which shows the surface concentrations of In and P (in percent of their cleaved InP surface concentrations) as a function of increasing Au coverage. The concentrations are obtained by integration of the In $4d$ and P $2p$ peak areas, taken by 70- and 175-eV photons, respectively. The initial drop in concentration corresponds to a uniform Au-InP interface without substantial interdiffusion, as compared with the AES findings. However, the SXPS and AES results can be reconciled by the low sputtering rate of InP, which causes a diffusional broadening of ~10 Å. At Au film thicknesses above 20 Å the In and P maintain relatively constant concentrations, the P more so and at a higher level than the In. The data of Figs. 5 and 7 are in good agreement if the "floating" P is taken into account. The excess P in the SXPS spectra (Fig. 7) should not be interpreted as a uniform distribution extending into the Au overlayer.

Additional information regarding the microscopic distribution in the segregated layer can be obtained by SXPS measurements at different photon energies, corresponding to different photoelectron escape depths. Table I summarizes these results, which are taken on the cleaved surface on 20- and 50-Å-thick Au films, as well as on the latte film after mild annealing. The ratios represent the peal areas taken at 130 and 100 eV for the Au $4f$ peak, at 175 150, and 140 eV for the P $2p$ peak, and at 70 and 40 e photon energies for the In $4d$ peak. These energie represent estimated probing depths of 2—4 and 6—8 Å respectively, and 10—15 Å for the 140-eV photons used t probe the P $2p$ level.[29] All areas are normalized to th most surface-sensitive peak area, which is taken as unity These areas can be compared with the data shown in Fig 5. Thus, the Au peak area ratio is $1:\frac{1}{2}$ at 20 Å coverage while at 50 Å coverage the Au signal below the surfac exhibits a relative increase and has the same area as th "surface" peak. This is in accordance with the segrega tion data for Au given in Figs. 5(b) and 5(d), i.e., th segregated In and P decrease the surface Au concentra tion. The In ratio shows that at depths of 6—8 Å fron the free-Au surface there is a higher In concentration tha at the surface itself, referred to the cleaved-surface ratic The same trend is seen in the P data, but probing deepe (10—15 Å) using 130-eV photons shows a decrease rela tive to the cleaved-surface ratio. This hints at the possi bility that the 10-Å-thick segregated layer of In and P o the Au film actually has a spatial distribution whic peaks at around a depth of 5 Å, decreases towards th free-Au surface, and falls off towards the film "bulk.

TABLE I. SXPS peak intensity ratios for Au $4f$, In $4f$, and P $2p$ core levels (columns 2—4) for different surface coverage (colum 1) taken at their respective photon energies (in parentheses in eV). Corresponding photoelectron escape depths appear in row 5.

Surface coverage	$I^{4f}_{\mathrm{Au}}(130)/I^{4f}_{\mathrm{Au}}(100)$	$I^{2p}_{\mathrm{P}}(175)/I^{2p}_{\mathrm{P}}(150)/I^{2p}_{\mathrm{P}}(140)$	$I^{4p}_{\mathrm{In}}(70)/I^{4p}_{\mathrm{In}}(40$
Cleaved InP(110)		1:12:12	1:1
Cleaved + 20 Å Au	$1:\frac{1}{2}$	1:13:8	1:2
Cleaved + 50 Å Au	1:1	1:15:10	1:2.2
Cleaved + 50 Å Au + annealing	1:2	1:18:30	1:2
Escape depth (Å)	2—4/6—8	2—4/6—8/10—15	2—4/6—8

The microscopic details at the surface cannot be yielded by AES data due to the fixed escape depth of the Auger electrons. This particular surface behavior is not entirely clear at the present time.

Subsequent mild annealing of the 50-Å-thick Au film causes an increase in the Au 4*f* peak area (not shown), an increase of the In 4*d* peak, and a decrease of the P 2*p* peak areas. The variable photon-energy results in Table I suggest that the annealing causes a broadening of the segregated P layer with a preferential loss of surface P, while the surface Au concentration increases. Simultaneously, somewhat more In out-diffuses to the free surface during the annealing process.

A similar segregation and interdiffusion pattern, as encountered in the gold films, is repeated with other unreactive metals.[30] Figure 8 is an example of a sputter-depth profile taken from a 60-Å-thick Cu film deposited on a UHV-cleaved (110) surface. Copper is relatively unreactive with InP.[8] Some differences are noted compared with Au: The In segregation is less evident, the P concentration in the Cu film is higher, and the Cu in-diffusion is deeper. Regarding the first difference, it is not clear whether the particular pattern of surface distribution reflects the conclusion obtained from the SXPS segregation data. Also, it is not clear whether the anion accumulation at the interface is not an artifact of the sputter-profile data acquisition. This effect is not repeated in thinner Cu films and therefore could reflect an enhanced drive-in effect of the phosphorus in the copper film. As in the Au films, the In and P segregation pattern does not become evident for Cu thicknesses below 20—30 Å.

Dramatic changes in the In and P out-diffusion and segregation patterns at the Au-InP interface are caused by very thin interlayers of reactive metals.[10] Figure 9 is a sputter-depth profile taken from a 70-Å-thick Au film deposited on a 2-Å-thick Al interlayer on a UHV-cleaved InP(110) surface. The $\geq$ 1-ML Al interlayer (ML denotes monolayer) is the only difference in experimental conditions between Figs. 9 and 5(d), but the P segregation is still totally eliminated. Similar experiments with Al thicknesses of 5, 10, and 20 Å yield the same result. The In out-diffusion does not seem to be affected by the interlayer. Unfortunately, the Au and Al Auger peaks fall at approximately the same energy and could not be resolved; thus the exact interlayer distribution cannot be seen. However, judging from results of other reactive interlayers shown later, it seems that the Au in-diffusion is also unaffected by the interlayer presence.

A similar experiment was carried out using SXPS in order to probe the initial steps of the interface formation. Figure 10 shows the In 4*d* photoemission spectra taken

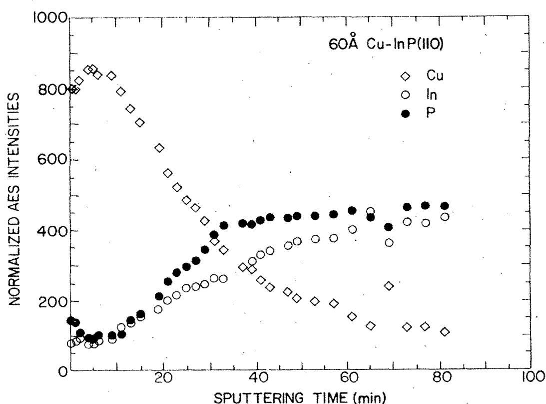

FIG. 8. AES depth profiles of Cu (triangles), In (solid circles), and P (open circles) from 60-Å-thick Cu film on a UHV-cleaved InP(110) surface.

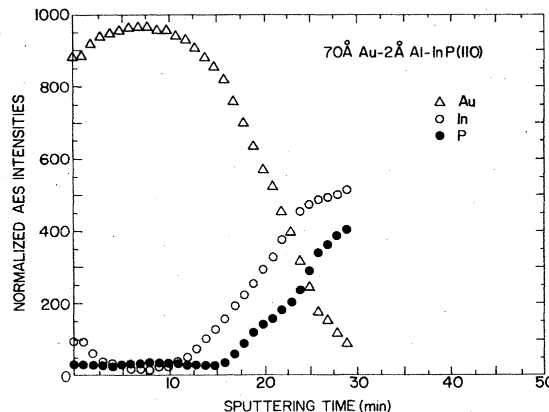

FIG. 9. AES depth profiles of Au, In, and P from a 70-Å-thick Au film on a 2-Å-thick Al interlayer on a UHV-cleaved InP(110) surface.

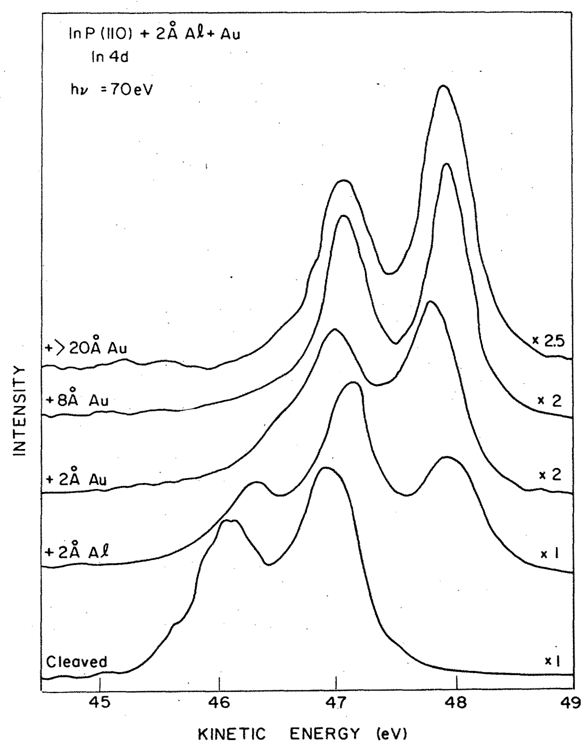

FIG. 10. Soft-x-ray photoemission spectra of the In 4*d* core level as a function of increasing Au deposition on a 2-Å-thick Al interlayer on a UHV-cleaved InP(110) surface using $h\nu = 70$ eV.

using 70-eV photons from a UHV-cleaved surface, with 2-Å Al coverage and subsequent Au coverage with increasing thickness. Deposition of 2 Å of Al causes a 0.3-eV shift of the bulk In 4d level superimposed on a 0.7-eV-shifted In 4d level of the dissociated In. Subsequent Au deposition leaves the dissociated peak only. The surface P was monitored by observing the P 2p photoemission spectrum. Such SXPS measurements are given in Fig. 11, which was taken, using 175-eV photons, from a UHV-cleaved surface before and after 2-Å Al deposition. The latter case shows considerable broadening of the peak, indicative of surface reaction with Al. Subsequent Au deposition causes the P 2p photoemission to fall below the detectable level.

In order to focus on the reactive-metal interfacial reaction, SXPS measurements were performed on InP(110) surface covered with increasing Al film thicknesses. Figure 12 shows the In 4d photoemission spectra taken by 70-eV electrons from a UHV-cleaved (110) surface covered with an increasing Al film thickness. Even at the very early stages of Al deposition, one can observe the initial 0.3-eV shift, apparently due to band bending, superimposed on the shifted In 4d peak, indicating dissociated In. These results suggest that the metallic, dissociated In "floats" on top of the reacted Al-P layer, segregating to its surface, in agreement with our AES results. Furthermore, the observation of the In core level associated with InP even after 8-Å Al deposition strongly suggests that the reacted layer may be discontinuous.

Further information about the reacted interfacial layer may be obtained from Fig. 13, which shows the Al 2p photoemission spectra taken by 130-eV photons from a UHV-cleaved InP(110) surface covered with increasing thicknesses of Al. At low coverages the Al core level is shifted towards higher binding energies, strongly pointing

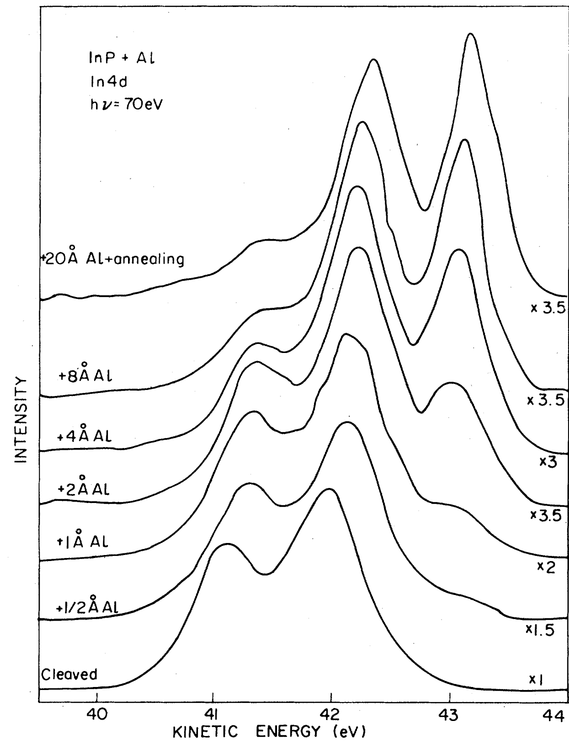

FIG. 12. Soft-x-ray photoemission spectra of the In 4d core level as a function of increasing Al deposition on a UHV-cleaved InP(110) surface using $h\nu = 70$ eV.

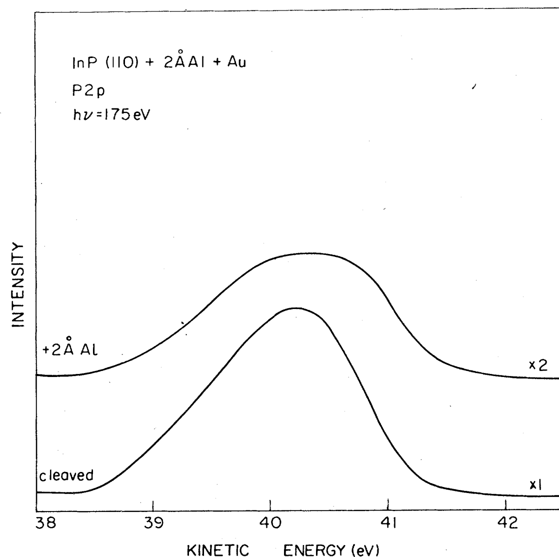

FIG. 11. Soft-x-ray photoemission spectra of the P 2p core level on a UHV-cleaved InP(110) surface before and after 2-Å-thick Al film deposition using $h\nu = 175$ eV.

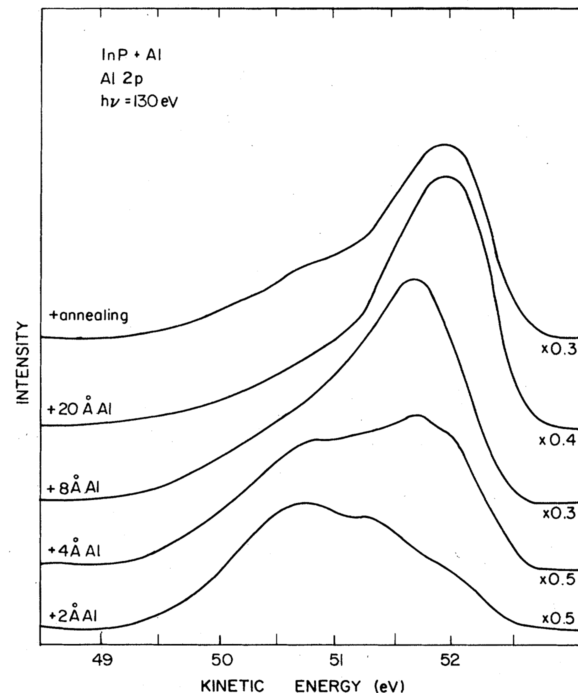

FIG. 13. Soft-x-ray photoemission spectra of the Al 2p core level as a function of increasing Al deposition on a UHV-cleaved InP(110) surface using $h\nu = 70$ eV.

to Al-P reaction which forms the thermodynamically favorable Al-P compound. At coverages below a monolayer, cluster formation may also shift the Al $2p$ peak to higher binding energies.[31] Subsequent depositions show the evolution of spectra in which the metallic Al core level emerges. It should be noted that a mild heat treatment increases the reacted Al "shoulder" (topmost spectrum), indicating a thicker Al-P layer induced by annealing. This is consistent with recent LEED and AES work of Kahn *et al.*[32]

The joint AES and SXPS results suggest a reaction of the Al interlayer with the surface excess P, which forms an Al-P compound. This "chemical trapping" of P creates a layer which may even be discontinuous, but proves to be an excellent barrier for additional P out-diffusion. Indium is able to diffuse through the reacted layer to segregate at the free-Au surface. The effect on Au in-diffusion is difficult to perceive at such low Al coverages.

More conclusive support for this process can be given by reactive metals, other than Al, the AES peaks of which can be distinguished from those of Au. Figure 14 is a sputter-depth profile of a 70-Å Au film on a 10-Å Ti interlayer deposited on a UHV-cleaved InP surface. Again, a total elimination of P out-diffusion and segregation is noted. The In seems to be unaffected by the interlayer. As the interface is approached, the Ti *LMM* peak rises, while the P peak, which has a smaller electron escape depth, lags somewhat behind. The latter seems to stabilize at a certain level, indicative of a compound formation, in the Ti film. The Au peak also shows a saturated level in the Ti film, indicating a certain solubility in the reacted layer. Further into the interface, the In and P rise to their bulk levels, while Au shows definite signs of in-diffusion, as in the Al interlayer case. A similar result was obtained with a 5-Å-thick Ti interlayer, the difference being a small signal of segregated P at the free-Au surface in this case.

Figure 15 shows an Auger sputter profile of another 70-Å-thick Au layer on a UHV-cleaved InP surface with a 20-Å-thick Ni interlayer. Again, the reactive interlayer proves to be an effective barrier for P out-diffusion, chemically trapping it at the interface, while the In is unperturbed from following the same out-diffusion trend. However, the Ni interlayer seems to also be a very strong diffusion barrier for Au, unlike the Ti case. The deeper Ni concentration "tail" may indicate stronger drive-in effects in this case.

In view of the results yielded by reactive-metal interlayers, it is interesting to note that a 20-Å-thick Cu interlayer between the Au film and the InP(110) surface gives the Auger sputter profile shown in Fig. 16. The interdiffusion and segregation patterns seem to be identical to the pure-Au case. A comparison of Figs. 12 and 13 leads to a realization of the importance of interlayer reactivity in determining the interface and free-surface chemical composition.

The type of metal interlayer is not the only important factor in determining interdiffusion. In this study we have focused on UHV-cleaved surfaces. If these surfaces are ion-bombarded prior to metal deposition, the results

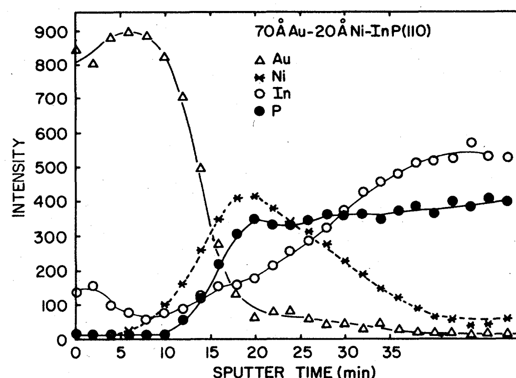

FIG. 15. AES depth profiles of Au, Ni, In, and P from a 70-Å-thick Au film on a 20-Å-thick Ni interlayer on a UHV-cleaved InP(110) surface.

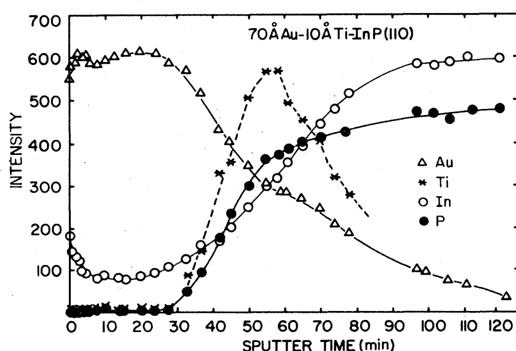

FIG. 14. AES depth profiles of Au, Ti, In, and P from a 70-Å-thick Au film on a 10-Å-thick Ti interlayer on a UHV-cleaved InP(110) surface.

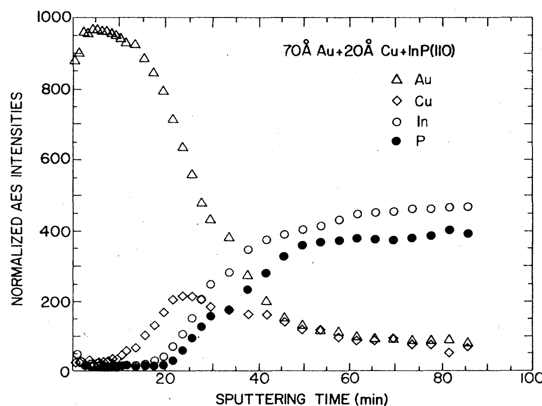

FIG. 16. AES depth profiles of Au (triangles), Cu (squares), In (solid circles), and P (open circles) from a 70-Å-thick Au film on a 20-Å-thick Cu interlayer on a UHV-cleaved InP(110) surface.

are markedly different. Figure 17 is a sputter-depth profile of a 70-Å-thick Au film on a 10-Å-thick Al interlayer deposited on an Ar^+-ion bombarded InP(110) surface. The In and P are distributed throughout the Au film, probably due to a mixture of out-diffusion and film discontinuity. No segregation pattern is evident and the interface seems to be very extended. This enhanced interdiffusion due to ion sputtering of the InP substrate is in agreement with results obtained for Al-Si interfaces.[33]

IV. DISCUSSION

The results obtained by Auger depth profiling highlight the power of this technique in obtaining important information about atomic spatial distribution at metal-semiconductor interfaces *after* the junction is prepared. The inherent interpretational difficulties of AES are avoided by performing a series of many experiments under identical conditions. Complementary to SXPS measurements, Auger sputtering profiling reveals in-depth information about the microscopic spatial distribution of the atomic components starting at the metal surface and continuing through the film to the metal-semiconductor interface and the InP bulk.

The results indicate that UHV-cleaved InP(110) surfaces are P-rich. Such effects have also been observed on cleaved GaAs surfaces.[34] The P-rich surfaces are affected in a dramatically different way by unreactive and reactive metals. The results show that Au as a representative of the former group seems to sink into the topmost layers, dissociating the lattice without reacting with it. The dissociated In and P tend to segregate to the top of the Au film and maintain that position apparently by microdiffusion simultaneously with the deposition process. Increasing thickness of the Au films shows no detectable P content, but does show various low concentrations of In diffused throughout the Au film itself. This is in accordance with the published solid solubilities of P and In in Au.[27] The variance in In concentration could be due to small differences in substrate temperature during deposition. However, the pattern of the In and P surface segregation appears to gradually decrease as a function of the

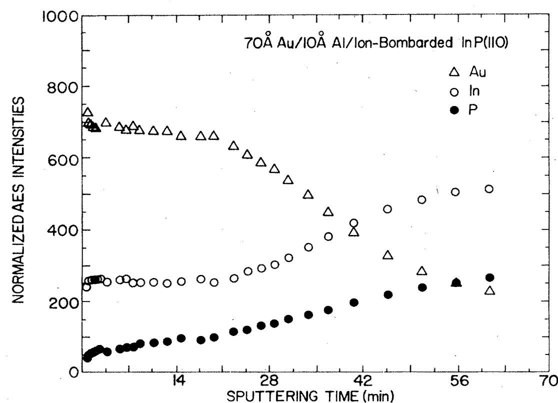

FIG. 17. AES depth profiles of Au, In, and P from a 70-Å-thick Au film on a 10-Å-thick Al interlayer on an Ar^+-ion-bombarded InP(110) surface.

metal-film thickness, especially for thicknesses above 30 Å. Below this value the segregation pattern may be screened by the inherent Auger electrons' escape depth or it may be insignificant due to the segregated layer width itself. For segregated layers thinner than the overlayers, the effect may cause misinterpretation of SXPS data, especially those taken at higher coverages and a single wavelength.

A survey of the results for the various thicknesses of Au films leads us to the conclusion that the Au-InP interface is 10—20 Å thick,[26] and that for Au films above that thickness there is a formation of a segregated layer of dissociated In and P about 10 Å thick at the free surface. This segregated layer has a peculiar spatial distribution—namely that the dissociated elements may reach their peak concentration slightly ($\sim$5 Å) below the surface proper.

A very different pattern of out-diffusion is observed in the case of reactive-metal deposition. These metals, exemplified by our results with Al, Ni, and Ti, tend to remain on the cleaved surface, and to react strongly with the phosphorus. This reacted layer creates a strong diffusion barrier for P which is chemically trapped at the interface. However, the out-diffusion of atomic In is not perturbed by the reacted layer. The reacted layer itself can be made very thin (several angstroms only) and may not even be continuous, but it is apparently a very effective chemical trap even if used as an extremely thin interlayer. If the reactive-metal interlayer is discontinuous it is probably so on a microscopic scale. This is emphasized by the results on the Ar^+-ion-bombarded surface, where the effects of the interlayer as a barrier are eliminated (see Fig. 17).

Thus the results on reactive- and unreactive-metal—InP interfaces demonstrate the importance of the chemical and physical interactions in determining the spatial distribution of the constituents over the formed junction. The unreactive metals appear to "sweep" the excess P to the free-metal surface and thus leave a P-depleted interface. This type of interface has been shown to have higher Schottky-barrier heights[9] and surface-state concentrations at the reported Fermi-level—pinning positions for such barriers.[11,35] The reactive-metal interfaces, on the other hand, trap the anion by chemical reaction while allowing the In to diffuse out. Thus an In-depleted interface is created which can be associated with the lower Schottky-barrier heights reported for such junctions.[10,13]

Our results cannot identify a particular set of defects or other electrically active sites as being directly responsible for the reported Fermi-level positions. Calculations of energy levels for various surface defects have been reported by several research groups in recent years.[36,37] The calculations indicate a P vacancy (V_P) level in[36] or just below[37] the conduction band, an In vacancy (V_{In}) around midgap, and antisite defects (In_P and P_{In}) deep in the InP band gap.[36] Our results on unreactive metals could indicate V_P formation at the interface, but such a level cannot account for the reported higher Schottky-barrier heights at unreactive-metal interfaces. Similarly, the reactive-metal—interface results which can be associated with In depletion (V_{In}) are not consistent with the lower Schottky-barrier heights reported on such interfaces. The only level which appears to be consistent with AES,

SXPS, and electrical results could be the In_P level, where In occupies P sites which are vacated by anion segregation to the free-metal surface. One should, however, bear in mind that these calculations are based on an assumed free, relaxed surface which may be very far from the disrupted, interdiffused interface, even in the nonreactive-metal case. For the possibility of Schottky barrier determination by interfacial defects, many possibilities exist—including native defects, impurities, and complexes thereof. However, for want of more adequate theoretical treatment, we therefore limit our conclusions to the role of the metal reactivity in determining the electrical parameters of the junction. This role seems to be dominant even at extremely low coverages on the UHV-cleaved surfaces.

ACKNOWLEDGMENTS

We wish to thank Dr. C. F. Brucker for designing the computer program used for acquiring depth profiles and for many productive discussions. We also thank Dr. H. Richter for valuable refinements to the data-analysis routines. We gratefully acknowledge J. Iseler (Lincoln Labs) for supplying the InP crystals and Jim Zesch (Xerox Palo Alto Research Center) for orientating and cutting them. This work was supported in part by the Office of Naval Research under Contract No. N00014-80-C-0778 (G.B. Wright). One of us (Y.S.) is grateful to the Belfer Center for Energy Research and the Israel Ministry of Energy for their support.

---

[*]On sabbatical leave from the Faculty of Engineering, Tel-Aviv University, Ramat Aviv 69978, Israel.

[1]L. Messick, D. L. Lile, and A. R. Clawson, Appl. Phys. Lett. **32**, 494 (1975).

[2]K. Kamimura and Y. Sakai, Thin Solid Films **56**, 215 (1979).

[3]L. G. Meiners, D. L. Lile, and D. A. Collins, J. Vac. Sci. Technol. **16**, 1458 (1979).

[4]D. L. Lile and M. J. Taylor, J. Appl. Phys. **54**, 260 (1983).

[5]K. Hattori and Y. Izumi, J. Appl. Phys. **52**, 5699 (1981).

[6]P. Sheldon, R. K. Ahrenkiel, R. E. Hayes, and P. E. Russel, Appl. Phys. Lett. **41**, 727 (1982).

[7]A. Heller and R. G. Vadimsky, Phys. Rev. Lett. **46**, 1153 (1981).

[8]R. H. Williams, V. Montgomery, and R. R. Varma, J. Phys. C **11**, L735 (1978).

[9]R. H. Williams, R. R. Varma, and V. Montgomery, J. Vac. Sci. Technol. **16**, 1418 (1979).

[10]L. J. Brillson, C. F. Brucker, A. D. Katnani, N. G. Stoffel, and G. Margaritondo, J. Vac. Sci. Technol. **19**, 661 (1981).

[11]Y. Shapira, L. J. Brillson, and A. Heller, J. Vac. Sci. Technol. A **1**, 766 (1983).

[12]P. W. Chye, I. Lindau, P. Pianetta, C. M. Garner, C. Y. Su, and W. E. Spicer, Phys. Rev. B **18**, 5545 (1978).

[13]L. J. Brillson, C. F. Brucker, A. D. Katnani, N. G. Stoffel, and G. Margaritondo, Appl. Phys. Lett. **38**, 784 (1981).

[14]A. McKinley, A. W. Parke, and R. H. Wiliams, J. Phys. C. **13**, 6723 (1980).

[15]D. L. Kirk and C. Jones, J. Phys. D **12**, 651 (1979).

[16]S. Singh, R. S. Williams, L. G. Van Uitert, A. Schlierr, J. Camlibel, and W. A. Bonner, J. Electrochem. Soc. **129**, 447 (1982).

[17]L. J. Brillson, Surf. Sci. Rep. **2**, 123 (1982).

[18]E. Hökelek and G. Y. Robinson, Solid State Electron. **24**, 99 (1981).

[19]B. L. Smith, J. Phys. D **6**, 1358 (1973).

[20]R. H. Williams and J. T. McGovern, Surf. Sci. **51**, 41 (1975).

[21]R. S. Williams, R. J. Nelson, and A. R. Schlierr, Appl. Phys. Lett. **36**, 827 (1980).

[22]D. K. Skinner, J. G. Swanson, and C. V. Haynes, Surf. Interface Anal. **5**, 38 (1983).

[23]Y. Shapira and L. J. Brillson, J. Vac. Sci. Technol. B **1**, 618 (1983).

[24]L. J. Brillson, Y. Shapira, and A. Heller, Appl. Phys. Lett. **43**, 174 (1983).

[25]W. E. Spicer, P. W, Chye, P. R. Skeath, C. Y. Su, and I. Lindau, J. Vac. Sci. Technol. **16**, 1422 (1979).

[26]L. J. Brillson, C. F. Brucker, N. G. Stoffel, A. D. Katnani, and G. Margaritondo, Phys. Rev. Lett. **46**, 838 (1981).

[27]M. Hansen and K. Anderko, *Constitution of Binary Alloys* (McGraw-Hill, New York, 1958).

[28]I. A. Babalola, W. G. Petro, T. Kendelewicz, I. Lindau, and W. E. Spicer, J. Vac. Sci. Technol. A **1**, 762 (1983).

[29]M. P. Seah and W. A. Dench, Surf. Interface Anal. **1**, 2 (1979).

[30]L. J. Brillson, Phys. Rev. Lett. **40**, 260 (1978).

[31]T.-X. Zhao, R. R. Daniels, A. D. Katnani, G. Margaritondo, and A. Zunger, J. Vac. Sci. Technol. E **1**, 610 (1983).

[32]A. Kahn, C. R. Bonapace, C. B. Duke, and A. Paton, J. Vac. Sci. Technol. B **1**, 613 (1983).

[33]L. J. Brillson, M. L. Slade, A. Katnani, M. Kelly, and G. Margaritondo, Appl. Phys. Lett. **44**, 110 (1984).

[34]W. Mönch, Thin Solid Films **104**, 285 (1983).

[35]H. Tempkin, B. V. Duff, W. A. Bonner, and V. G. Keramidas, J. Appl. Phys. **53**, 7529 (1982).

[36]J. D. Dow and R. E. Allen, J. Vac. Sci. Technol. **20**, 659 (1982).

[37]M. S. Daw and D. L. Smith, Appl. Phys. Lett. **36**, 690 (1979); Phys. Rev. B **20**, 5150 (1979).